Precast concrete sandwich wall panels with bolted angle connections tested in flexure under simulated wind pressure and suction

Nathan Teixeira, Douglas G. Tomlinson, and Amir Fam

- Flexural tests were performed on precast concrete sandwich wall panels with various end support conditions, loading orientations, and reinforcement and shear connector materials.
- Panels with steel and basalt-fiber-reinforced polymer (BFRP) longitudinal reinforcement were tested and compared. Discrete steel and BFRP shear connectors were also evaluated.
- In all cases the bolted connections succeeded in developing the full strength of the sandwich wall panels. Panels with steel reinforcement failed due to rupturing of flexural reinforcement, while a panel with BFRP reinforcement failed due to rupturing of shear connectors and crushing of concrete in one wythe.

A growing emphasis on energy efficiency in the erection and operation of buildings has resulted in a trend toward developing new construction techniques and improving current methods. Integrally insulated concrete wall panels have been in use for roughly 50 years and represent a feasible solution to energy-efficient construction. These precast concrete sandwich wall panels are typically composed of two concrete layers separated by an insulating layer of rigid foam.[1] In addition to providing a wide range of thermal resistance, the insulating foam also transfers a portion of shear forces between concrete layers.[2] The structural performance of a sandwich wall panel is ultimately governed by the degree to which shear is transferred between wythes.[3] Many shear transfer methods have been proposed and investigated in the past two decades in an attempt to achieve maximum composite action between wythes while maintaining thermal efficiency. Although full composite action is ideal with regard to structural performance, partial composite action with incomplete shear transfer is the reality.[4] In terms of shear connection mechanisms, steel connectors are the conventional choice due to their affordability and availability. However, fiber-reinforced polymers (FRPs) have become the focus of new research in the area of shear connection. An advantage of using certain FRPs is their greater tensile strength relative to steel as well as lower thermal bridging between wythes. Although steel is a mechanically

Table 1. Test matrix

Specimen	Flexural reinforcement material	Shear connector material	Loading direction	Boundary support condition	Concrete compressive strength f_c', MPa
W1	Steel	Steel	Pressure	Bolted connections	69.4
L1*	Steel	Steel	Pressure	Rollers	57.4
W2	Steel	Steel	Suction	Bolted connections	60.1
L2*	Steel	Steel	Suction	Rollers	63.0
W3	BFRP	BFRP	Pressure	Bolted connections	64.8
L3*	BFRP	BFRP	Pressure	Rollers	61.0

Note: BFRP = basalt-fiber-reinforced polymer. 1 MPa = 0.145 ksi.
* Data from Tomlinson and Fam (2015)

adequate connector material, thermal bridging induced by steel connectors diminishes a panel's thermal efficiency. The thermal bridging effect can reduce the panel's thermal performance by up to 40%.[5]

In the past decade, several glass-fiber-reinforced polymer and carbon-fiber-reinforced polymer shear connectors have been proposed, including a widely researched shear grid system.[6,7] Recently, basalt-fiber-reinforced polymer (BFRP) shear connectors have been investigated in an attempt to capitalize on the material's thermal benefits and tensile capacity. Naito et al.[8] assessed the strength and response of various shear connectors, including symmetrical diagonally oriented BFRP connectors. Tomlinson et al.[9] performed push-through and full-scale flexure tests on concrete sandwich panels with angled and horizontal discrete BFRP connectors.

Much of the research conducted on full-scale sandwich wall panels and precast concrete wall systems in general has involved the use of simple boundary conditions. In practice, connections with partial end fixity are more common. Pang,[10] Benayoune et al.,[11] and Carbonari et al.[12] have studied variations of cast-in-place concrete L-shaped connections with open and closed reinforcement loops for concrete sandwich panels. Pang[10] concluded that the L-shaped connections with closed loop reinforcement provided the most desirable behavior in terms of structural ductility and strength. Metelli and Riva[13] investigated the use of a novel steel hardware system for end connection. The researchers determined that the support system provided an adequate degree of energy dissipation and overall load resistance. However, these researchers did not explore the effect of the connection systems on the flexural behavior of concrete sandwich panels.

A widely used connection system in the precast concrete industry that has not been studied in conjunction with sandwich wall panels is the bolted angle. These connections allow for quicker erection times and higher tolerance levels for precast concrete panel construction.[14] This paper aims to investigate the effect of this connection system on the flexural behavior of sandwich wall panels in terms of strength and stiffness. Various parameters were investigated, including the direction of loading and reinforcement/shear connection material. An analytical model is proposed to predict the linear and nonlinear response of panels with various shear transfer mechanisms and types of end fixity.

Experimental program

Test matrix

A total of three parameters were examined in the testing program: flexural reinforcement and shear connector material, loading direction, and end support condition. **Table 1** summarizes the specimens and their corresponding parameters. Specimens W1 and W2 contained steel flexural reinforcement and shear connectors, while specimen W3 contained BFRP flexural reinforcement and shear connectors. Specimens W1 and W3 were loaded out of plane on the facade wythe to simulate external wind pressure in the windward direction. Conversely, specimen W2 was loaded out of plane on the structural wythe, simulating a leeward suction pressure. Specimens W1 to W3 were all supported by bolted angle connections to simulate practical end conditions. Table 1 also shows specimens L1 to L3, which are counterparts that are similar to specimens W1 to W3, respectively, except that they were supported by rollers during testing.[15]

Panel description

Figure 1 depicts the panels' cross sections and dimensions. Specimens W1 through W3 were 600 mm (24 in.) wide and 2700 mm (106 in.) long with a depth of 270 mm (11 in.). Each of the specimens had two 60 mm (2.4 in.) thick facade and structural wythes that encapsulated a 150 mm (6 in.) rigid sheet of expanded polystyrene. The structural wythe was designed as a T section with a 90 mm (3.5 in.) high web to reduce the shear transfer distance of the connectors through the

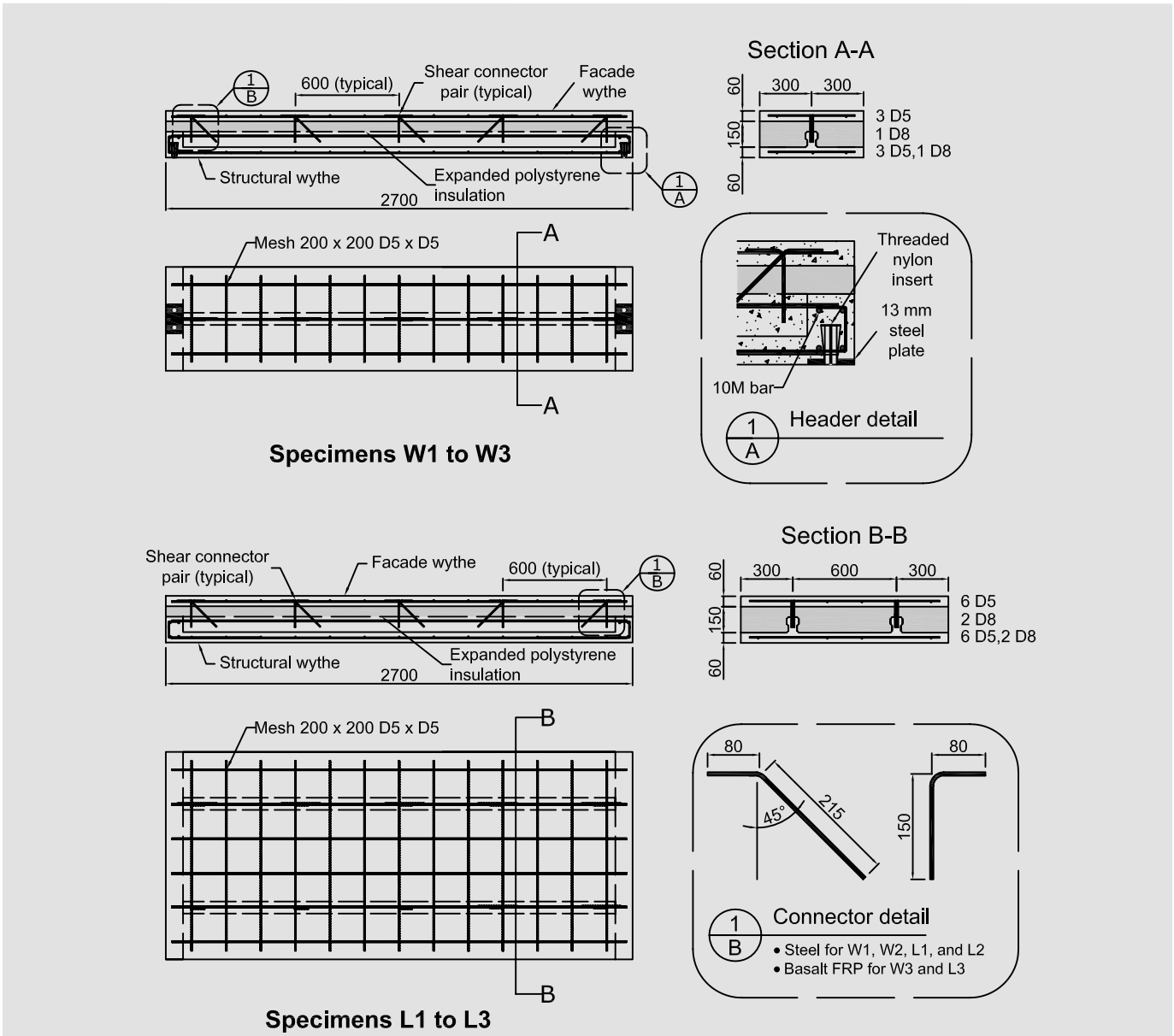

Figure 1. Schematic of test specimens. Note: All dimensions are in millimeters. EPS = expanded polystyrene; FRP = fiber-reinforced polymer. 10M = no. 3; D5 = 0.25 in.; D8 = 0.32 in. 1 mm = 0.0394 in.

insulation to 60 mm while avoiding a thermal bridge of solid concrete. A thickened concrete header and footer reinforced with four 10M (no. 3) bars were integrated with the structural wythe to facilitate loading and bearing in practice. Designed according to the American Concrete Institute's (ACI's) *Building Code Requirements for Structural Concrete (ACI 318-14) and Commentary (ACI 318R-14)*,[16] the wythes of specimens W1 and W2 were reinforced with a custom-welded wire mesh of 6.2 mm (0.24 in.) diameter deformed bars (D5 [gauge 3]) spaced at 200 mm (8 in.), with a total of three bars in specimens W1 and W2. An additi onal 8.1 mm (0.32 in.) diameter deformed steel bar (D8 [gauge 1/0]) was placed within the web as well as in the structural wythe beneath the web for added flexural resistance. For specimen W3, 6 mm (0.23 in.) diameter BFRP reinforcing bars were used to form a 200 × 200 mm mesh, constructed using plastic zip ties. Also, two additional 8 mm (0.31 in.) diameter BFRP bars were used, one in the web and one in the flange, as in specimens W1 and W2. Pairs of shear connectors were spaced longitudinally at 600 mm along the panel length. One leg of each shear connector pair was perpendicular to the wythe plane, while the other was inclined at a 45-degree angle to horizontal pointing away from the end of the panel. Orienting the angled legs in this manner produced a tensile force along the length of the connector when the panel was loaded in pressure and a compressive force when the panel was loaded in suction. For specimens W1 and W2, D5 steel bar was used for shear connectors, while 6 mm BFRP was specified for specimen W3. The BFRP connectors were cut from a rectangular spiral typically used for stirrups or column ties. Specimens L1 through L3 were identical to specimens W1 to W3, respectively, except that they were

1200 mm (47 in.) wide, essentially double the width of specimens W1 to W3, and each had two concrete webs (Fig. 1).

Two 19 mm (0.75 in.) diameter nylon threaded inserts were placed within the header and footer at the ends of the panels of specimens W1 to W3 to facilitate the attachment of bolted connections to the structural wythe. These inserts were 50 mm (2 in.) from the ends of the panel and 100 mm (4 in.) apart, centered on the longitudinal midline of the panel (Fig. 1). A 13 mm (0.51 in.) thick steel plate was used to encapsulate the threaded inserts, thereby maintaining proper embedment and spacing during concrete placement.

Fabrication

Sandwich wall panel construction began with the assembly of the reinforcing cage. The web reinforcement was positioned inside the expanded polystyrene sheet and held in place by circular chairs. The facade mesh was placed on chairs, which were then attached to the expanded polystyrene using large wire staples. The assembly was then gently flipped over and the structural wythe mesh was attached to the expanded polystyrene. The header reinforcement and threaded inserts were installed before the expanded polystyrene and reinforcement assemblage were positioned inside of the vertical forms (specimens W1, W2, L1, and L2). Concrete was then placed incrementally into each wythe space to maintain equal pressure. Specimens W3 and L3 were constructed at a later date and placed horizontally. Under this configuration, the facade wythe was placed initially, followed by the insertion of the expanded polystyrene and reinforcement assemblage before the placement of structural wythe concrete. After a 24-hour curing period, the panels were removed from the forms.

Materials

The concrete used in this test program was a self-consolidating mixture with 60 MPa (8700 psi) design strength. The D5 (gauge 3) steel bar used for the reinforcing mesh and shear connectors had a cross-sectional area of 31 mm^2 (0.048 $in.^2$), elastic modulus of 196 GPa (28,400 ksi), yield strength of 485 MPa (70,300 ksi), and ultimate strength of 650 MPa (94,300 ksi). Similarly, the D8 (gauge 1/0) steel bar had a cross-sectional area of 51 mm^2 (0.079 $in.^2$), with material properties identical to the D5 bar. The 6 and 8 mm (0.23 and 0.31 in.) diameter BFRP bars had cross-sectional areas of 28 and 59 mm^2 (0.043 and 0.091 $in.^2$), respectively, as determined by immersion tests. In tension, the BFRP had an elastic modulus of 70 GPa (10,000 ksi) and guaranteed ultimate strength of 1100 MPa (160 ksi). The insulating layer comprised 20 kg/m^3 (34 lb/yd^3) graphite-infused expanded polystyrene, which was precut to the desired shape and dimensions. Hot-dipped, 19 mm (0.75 in.) diameter ASTM A325[17] bolts with a tensile strength of 621 MPa (90 ksi) and shear strength of 414 MPa (60 ksi) were used for the connections. The bolts were secured through 200 mm (8 in.) wide, 127 × 127 × 13 mm (5.0 × 5.0 × 0.5 in.) mild structural steel angles with a grade of 350W (50 ksi). The nonshrink grout used in the assembly of the test setup (discussed next) had one- and three-day compressive strengths of 26 and 42 MPa (3800 and 6100 psi), respectively.

Test setup and instrumentation

A specially designed setup was used to accurately simulate the field condition of a sandwich wall panel spanning between two floors with a bolted angle connection to each floor. Reinforced concrete support blocks simulating the floor slabs were used (**Fig. 2**). The two blocks were tied together at the base using threaded rods to restrain any horizontal displacement. Each block consisted of two components: a reusable base section and a top section that was anchored to the base section using 19 mm (0.75 in.) diameter high-strength threaded rods and could be replaced if damaged during a test. The sandwich wall panels were connected to the top section of the supports using the bolted angle connections such that only the structural wythe bears against the block as in practice.

While the panels were lying horizontally, the angles were attached to them at each end using bolts such that the vertical leg of each angle was offset from the end of the panel by 6 mm (0.23 in.). This gap was filled with grout at a later stage at the interface between the structural wythe and the support block, as in practice between the panel and floor slab. The panel was then lowered into position between the end blocks, and the vertical legs of the angles were connected with bolts fastened into preexisting threaded steel inserts inside the upper support block. Then, the 6 mm gap between the support blocks and the ends of the structural wythe was grouted. Unlike specimens W1 and W3, specimen W2 was tested with the panel flipped over and the bolted angle connection on the top concrete surface (Fig. 2). Specimens L1 to L3 were simply supported by rollers at each end, producing a span of 2630 mm (104 in.) and constant shear zones of 1040 mm (40.9 in.) (Fig. 2).

Each of the test specimens was loaded in four-point bending using spreader beams to create a constant moment zone of 550 mm (22 in.) at midspan. The panels were loaded in stroke control at a rate of 2 mm/min (0.08 in./min) using a 223 kN (50 kip) hydraulic actuator. Each specimen was outfitted with five 100 mm (4 in.) linear potentiometers to measure deflection beneath the panel along the span length. In order to evaluate the effect of the bolted angle connections, a combination of three linear potentiometers was used at each end of specimens W1 through W3 to measure end rotations. During fabrication, 5 mm (0.2 in.) 120 Ω uniaxial strain gauges were attached to the reinforcing bars at midspan in the facade and structural wythes, as

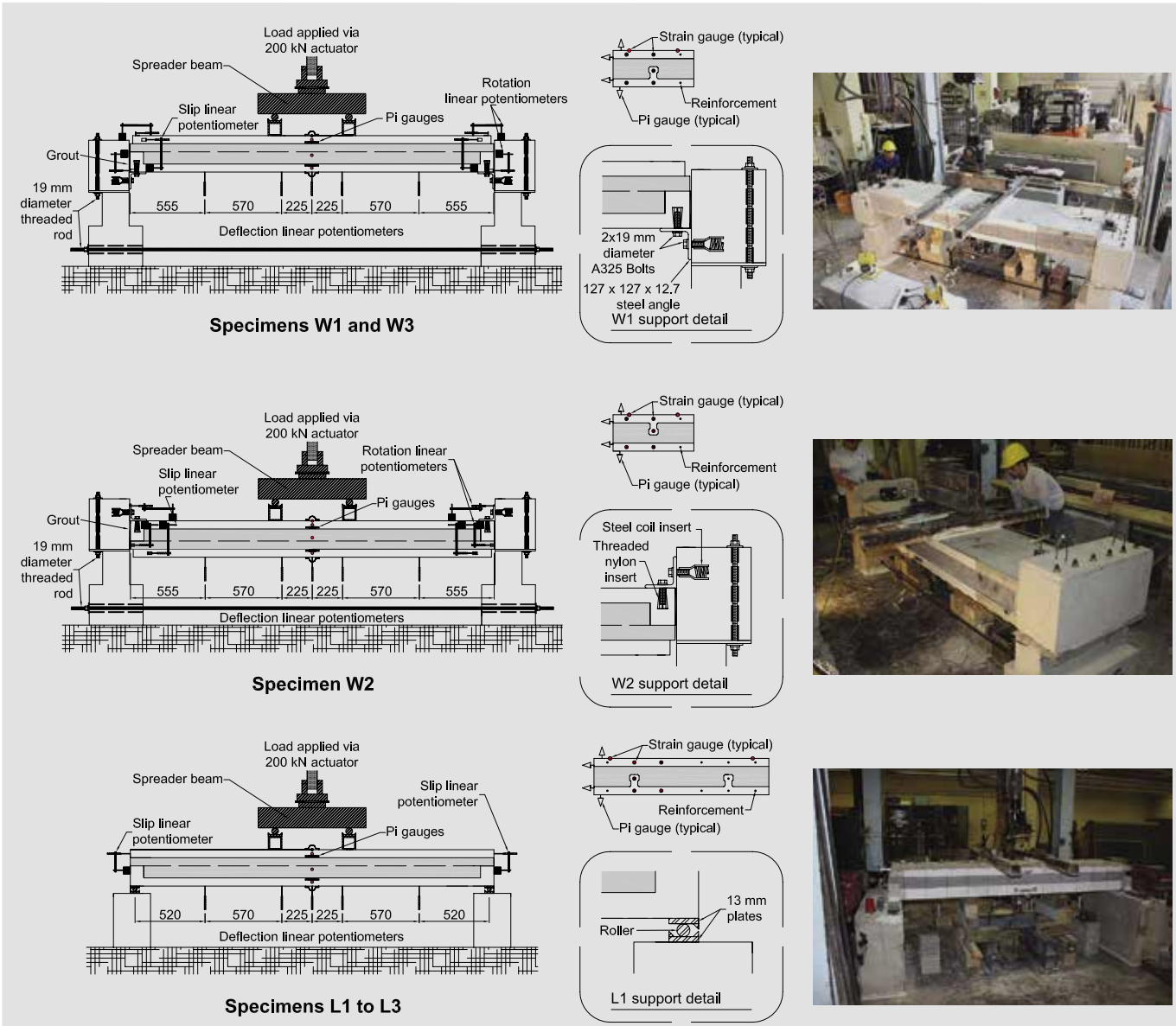

Figure 2. Test setup and instrumentation. Note: All dimensions are in millimeters. 1 mm = 0.0394 in.; 1 kN = 0.225 kip.

well as the web reinforcement. Before testing, two 50 mm (2 in.) 120 Ω uniaxial concrete strain gauges were adhered to the top concrete surface. Each specimen was also equipped with four 100 mm pi gauges along the depth of the midspan section to measure strain distribution. In addition, digital image correlation was employed to measure horizontal slip and end rotation. Sequential images were taken from two stationary 18-megapixel cameras at each panel end to determine the horizontal and vertical translation of textured surfaces between successive images.

Experimental results

This section discusses the experimental results in terms of load deflection, load-end slip, load-end rotation, load-strain responses, strain distribution, and failure modes. Various parameters affecting structural behavior are examined. The experimental load responses do not include the self-weight of the panels, which is equivalent to an applied load of 2.75 kN (0.618 kip). In addition, the load values for the responses of counterpart specimens L1 to L3 supported by rollers were divided in half because the cross sections were twice as wide as those of specimens W1 to W3.

Figure 3 illustrates the load-deflection responses at midspan. All responses are characterized by high initial stiffness followed by cracking and reduced stiffness before the peak load and onset of failure. **Table 2** summarizes the flexural cracking and peak loads. The onset of flexural cracking varied between panels as a result of support conditions, insulation-concrete bond strength, and preexisting shrinkage cracks. Specimens W1 and L1 (simulating wind pressure), which had identical characteristics other than support conditions, displayed similar behavior during testing. Yielding of the structural wythe reinforcement was followed by yielding of the web reinforcement. The load

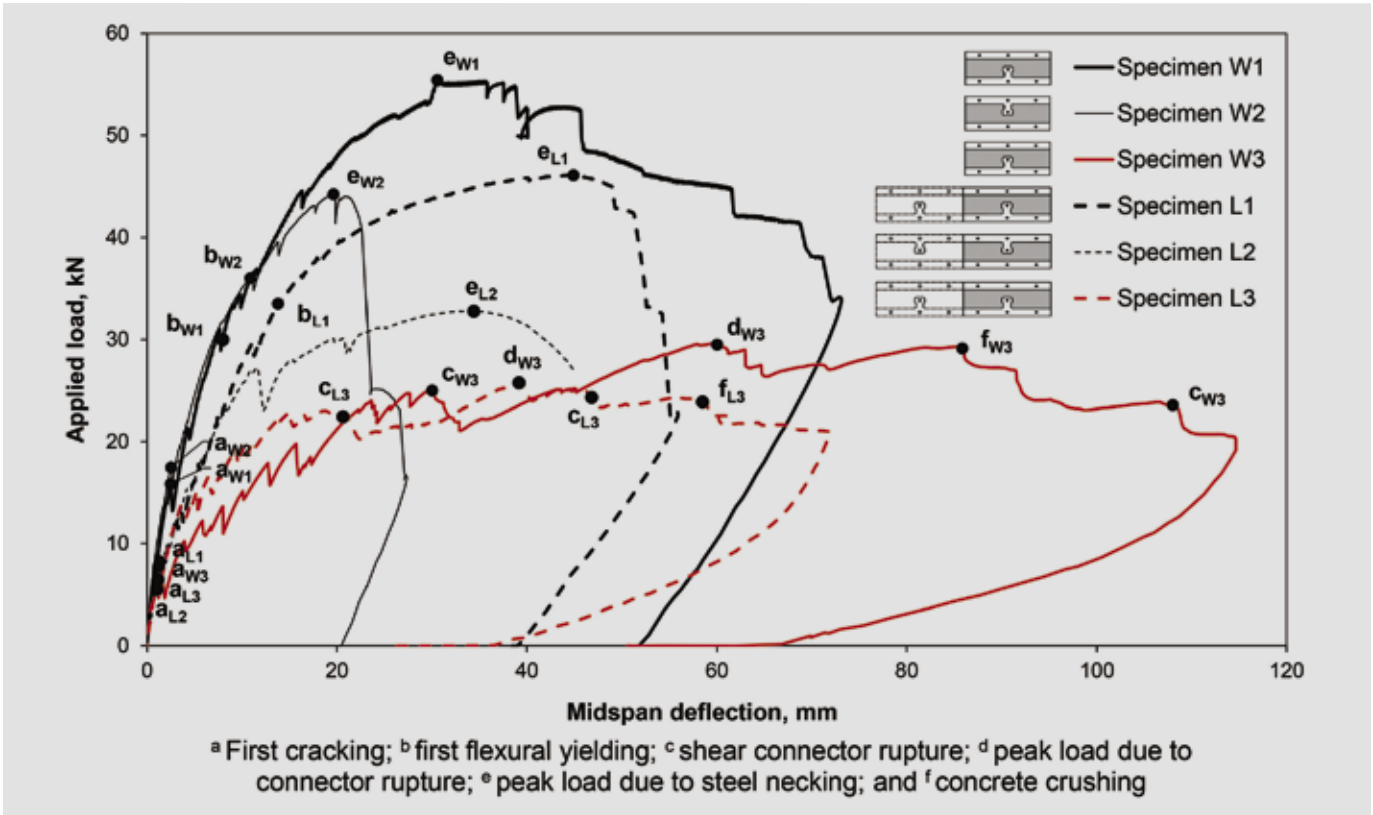

Figure 3. Load-midspan deflection relationship for each test specimen. Note: 1 mm = 0.0394 in.; 1 kN = 0.225 kip.

continued to increase marginally as the facade reinforcement underwent tension and the structural reinforcement entered the strain hardening phase. Soon thereafter, the load peaked as the bottom layer of reinforcement necked, followed by rupture and a sudden drop in load.

A similar series of events occurred in specimens W2 and L2 (simulating wind suction), though the less-reinforced

Table 2. Summary of experimental testing results

Specimen	Cracking load, kN	Peak load, kN	Midspan deflection at peak load, mm	Total end slip at peak load, mm	Average end rotation at peak load, degrees	Amount of composite action, %	Failure mode
W1	15.86	55.43	30.55	7.19	2.12	87.5	Longitudinal steel rupture
L1	7.79*	46.09*	44.90	7.08	2.52	81.3	Longitudinal steel rupture
W2	17.47	44.22	19.64	1.76	0.85	66.3	Longitudinal steel rupture
L2	5.53*	32.77*	34.40	1.87	n/a	57.1	Longitudinal steel rupture
W3	8.27	29.70	60.16	23.67	4.01	21.0	Shear connector rupture and concrete crushing
L3	6.47*	25.76*	39.16	16.43	3.61	29.4	Shear connector rupture and concrete crushing

Note: n/a = not applicable. 1 mm = 0.0394 in.; 1 kN = 0.225 kip.
* Half-width load

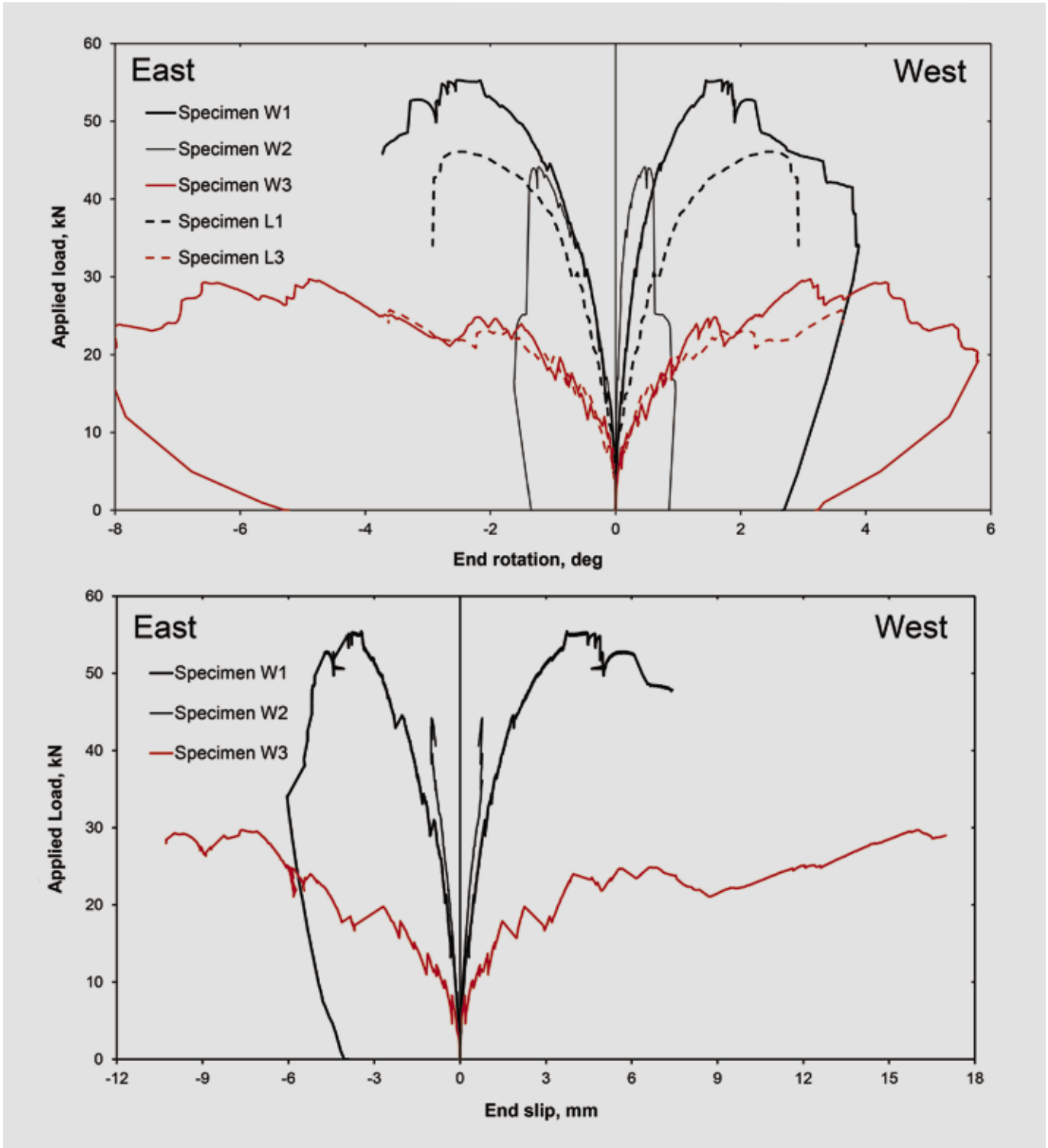

Figure 4. Load-end rotation (top) and load-end slip relationship (bottom) for all test specimens. Note: 1 mm = 0.0394 in.; 1 kN = 0.225 kip.

bottom (facade) reinforcement had a lower tensile resistance, leading to lower ultimate loads compared with specimens W1 and L1, respectively. The insulation-concrete bond for specimens W3 and L3 (simulating wind pressure and reinforced with BFRP) were noticeably weaker than other specimens because of the horizontal casting. Following cracking and a reduction in stiffness, the BFRP shear connectors underwent considerable shear deformation and eventually ruptured, lowering the amount of composite action between wythes. Following the rupture of the connectors, the concrete web crushed near midspan. The longitudinal BFRP reinforcement remained intact.

Figure 4 depicts the load-end rotation behavior at each end support of the panels. Data for specimen L2 were

not available, and rotation was measured at only one end of specimens L1 and L3. Because rotation and deflection are related through curvature, the shapes of the load-end rotation curves were similar to those of the corresponding load-deflection plots.

Figure 4 also shows the load-end slip responses at both ends of each test panel in this study, while Table 2 presents the total slip at peak load. Specimens W1 and W2 experienced comparable slips; however, specimen W3 exhibited significantly more slip as a result of poor insulation-concrete adhesion. Consequently, the majority of the shear transfer demand shifted to the shear connectors.

Figure 5 shows the load-strain responses of the three panels. Flexural cracking was evidenced by horizontal translations in the tensile reinforcement load-strain curves. The strain in the extreme top concrete fiber followed a similar trajectory for each of the test panels and underwent relatively low levels of compression. Specimen W3 was the only panel to experience concrete crushing in the web, as verified by the strain reaching approximately $-3500\ \mu\varepsilon$ at the level of the BFRP web reinforcement. Two distinct neutral axes were observed in each panel. Following cracking, the depths of the compressive zones were rather small due to the low reinforcement ratio. As specimens W1 and W3 reached their ultimate loads, the flanges of the structural wythes were fully cracked, as shown by positive strain values at the tops and bottoms of the flanges. The facade wythe of specimen W2 also experienced complete cracking. Figure 5 shows comparatively low strain values within the structural wythe of specimen W1 as the pi gauges did not intercept any flexural cracks.

Effect of support condition

This parameter can be assessed by comparing specimens W1 to W3 with angle connections with their specimen L1 to L3 counterparts, which are supported by rollers. The addition of bolted angles provided partial fixity at supports (Fig. 3 and 4), which led to greater stiffness and lower rotations at the same loads and also higher peak loads (Table 2). With the introduction of a negative moment at the supports, the structural demand in the constant moment zone was reduced, leading to a higher overall structural capacity. Although this effect was evident in steel-reinforced specimens W1 and W2, it was less pronounced in the BFRP-reinforced specimen, W3. This may be attributed to the significantly lower composite action of specimen W3.

Effect of loading direction

Figure 3 highlights the effect of loading direction, as evidenced by the peak load disparity between specimens W1 and W2. Following the cracking of concrete, both specimens exhibited a similar load-deflection response before the failure of specimen W2. Specimen W1 was inherently stronger than specimen W2 due to the higher reinforcement ratio in the region of highest tensile demand. Despite the diagonal shear connector legs undergoing compression rather than tension due to specimen W3's suction configuration, the overall panel stiffness was unaffected. Similar conclusions are drawn by comparing reference specimens L1 and L2.

Effect of flexural reinforcement and shear connector material

This parameter can be assessed by comparing specimens W1 and W3, which were both tested in a pressure configuration that had similar reinforcement ratios. Unfortunately, the different orientation during casting of both panels led to a weaker insulation-concrete bond in specimen W3 than in specimen W1, which was not intended. The stiffness of the load-deflection response and peak load of specimen W3 were significantly lower than those of specimen W1 (Fig. 3). The reduced stiffness was expected because the elastic modulus of BFRP (70 GPa [10,000 ksi]) was 2.8 times less than that of the deformed steel bar (196 MPa [28,400 ksi]) and the insulation-concrete bond was also somewhat weaker. Similar conclusions are drawn when comparing specimens L1 with L3.

Failure modes

Figure 6 shows different failure modes that occurred. Flexural cracking and longitudinal steel rupture occurred after excessive yielding, respectively, in pressure-loaded specimen W1. (Suction-loaded specimen W2 failed similarly to specimen W1.) BFRP shear connectors ruptured in pressure-loaded specimen W3, which was followed by concrete web crushing. The bolted angle at support permanently deformed after the failure of pressure-loaded specimens W1 and W3, suggesting yielding of the angle. The angle support region in suction-loaded specimen W2 experienced surface cracks at the ends, which are evidence of some negative moment near the support.

Analytical model

A model was developed to predict the flexural response of partially composite concrete sandwich wall panels with semi-rigid support conditions. An iterative process was developed using a global structural model of the system, including discrete bond-slip link elements to capture the partial composite action and nonlinear cracked-section analysis to develop the moment-curvature responses of the wythes for the purpose of identifying flexural stiffness and flexural failure events.

Structural analysis model

Figure 7 shows the actual configuration and idealized model layout of the sandwich wall panel. The two-

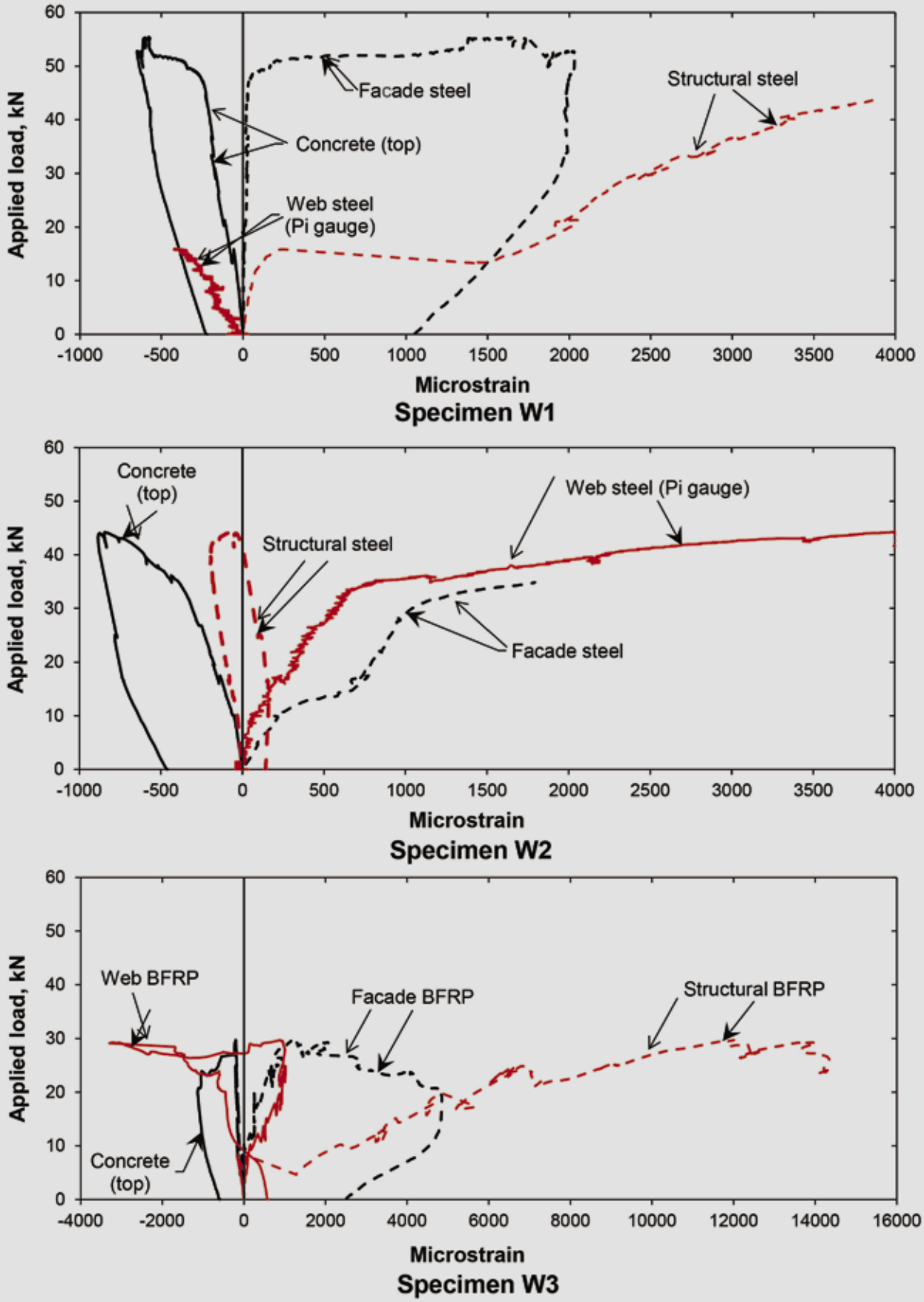

Figure 5. Load-strain relationship for each test specimen. Note: BFRP = basalt-fiber-reinforced polymer. 1 mm = 0.0394 in.; 1 kN = 0.225 kip.

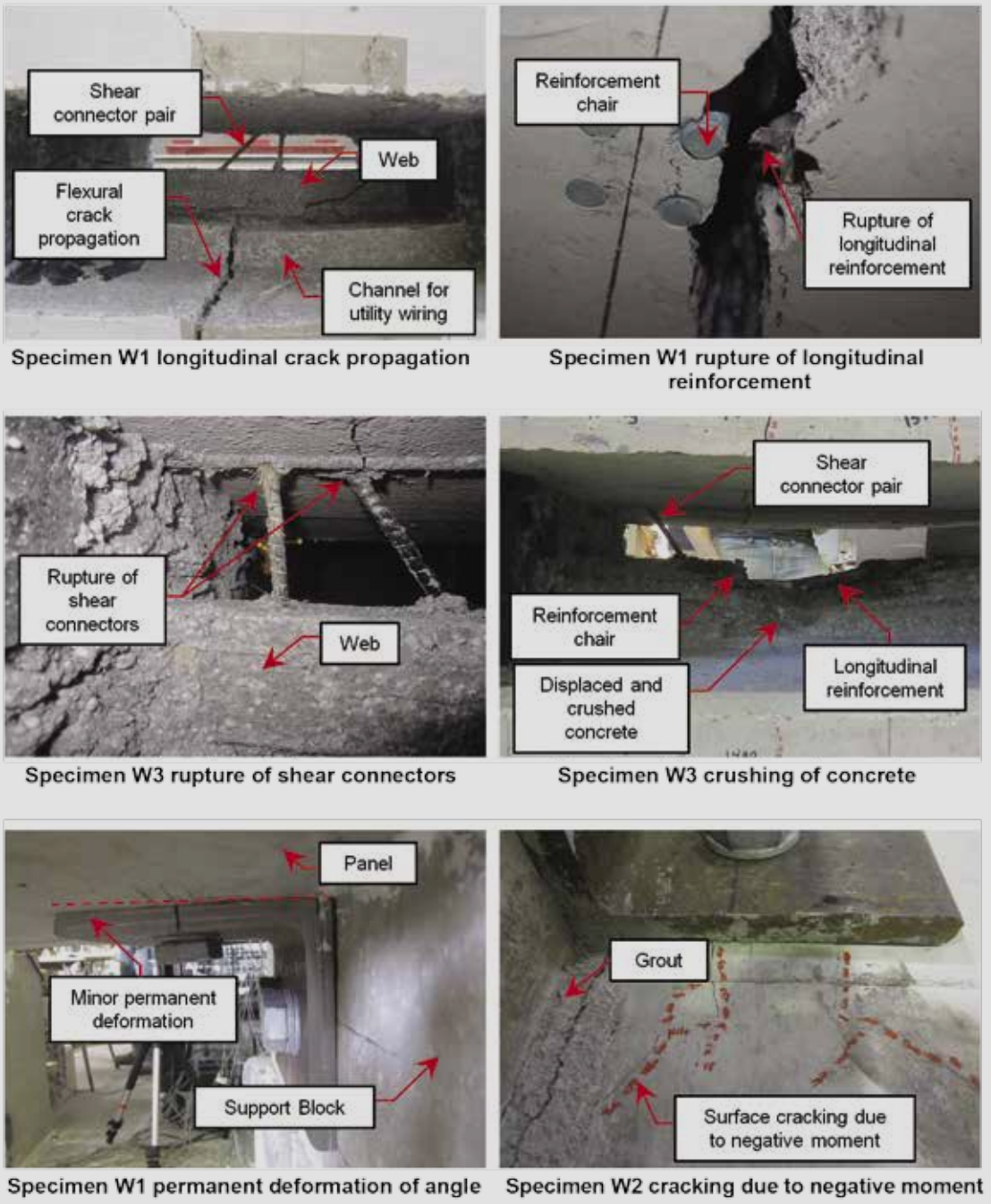

Figure 6. Various sandwich wall panel failure modes.

dimensional model was created using structural analysis software and comprises various components. Beam elements with equivalent square cross sections were used to represent the facade and structural wythes, along with maintaining the same distance between their respective centroids (cross section in Fig. 7). The remainder of the components primarily comprised joint links to define the force-deformation relationships. The semi-rigid bolted angle supports were modeled using hinged joint restraints overlaid with one-joint links assigned to apply rotational end stiffness $K_{e,i}$ about the local 3 axis (R3). The rigid foam insulation was modeled using two-joint links closely spaced at 30 mm (1.2 in.) increments horizontally along the span. The rigid foam (insulation) link was fixed vertically (direction U1) to ensure that the individual wythe beam elements deflected equally.

The other five degrees of freedom for this link (U2, U3, R1, R2, and R3) had an assigned stiffness value of zero. The shear transfer mechanism was composed of two types of link elements (Fig. 7). Two rigid arms (two-joint link elements), 30 and 110 mm (4.3 in.) long, respectively, were

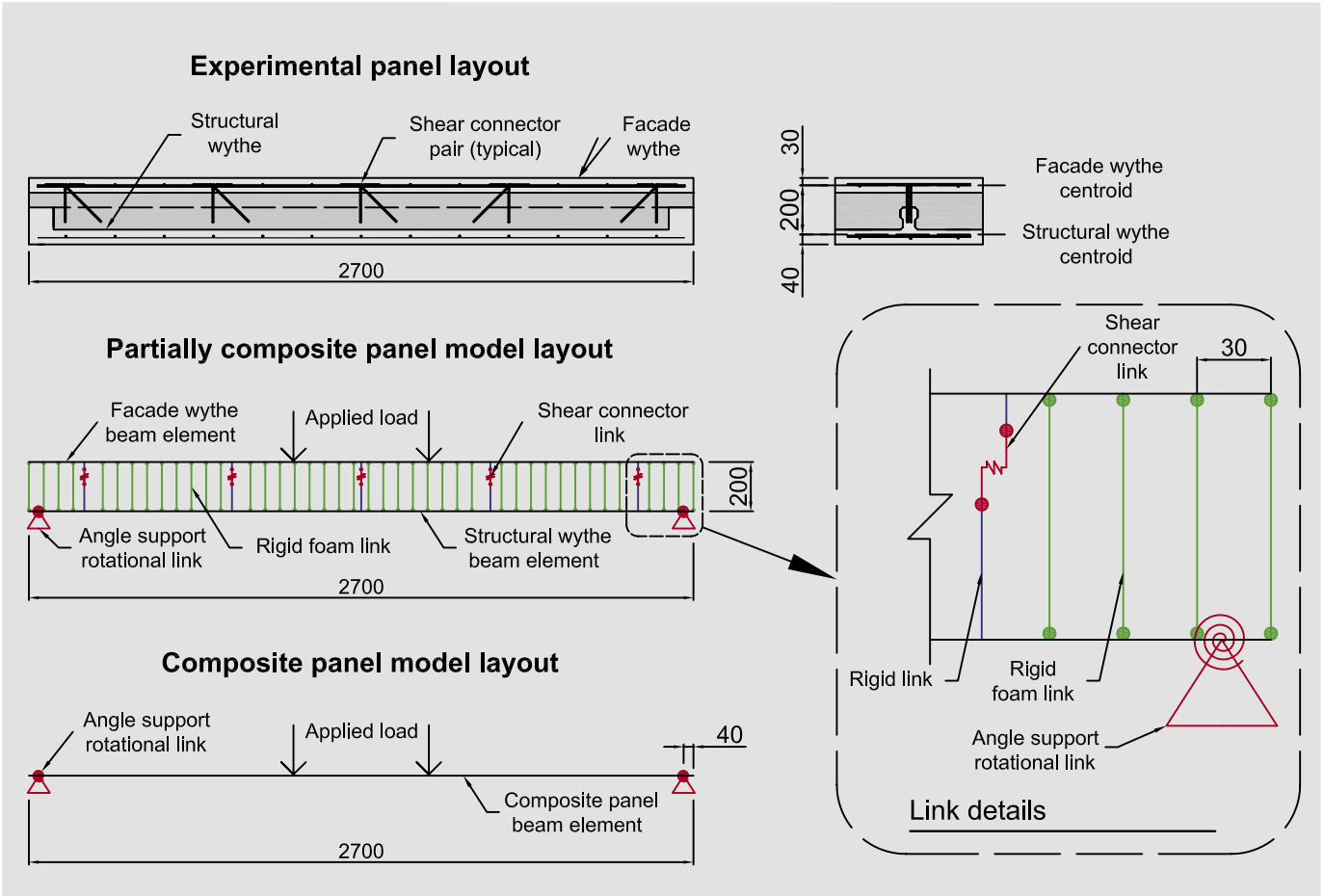

Figure 7. Actual and idealized structural analysis model layout of sandwich wall panel. Note: All dimensions in are millimeters. 1 mm = 0.0394 in.

employed to traverse the distance between the insulation-concrete interface and the centroid of each respective wythe. Because these members are solid concrete in actuality, they were modeled with six fixed degrees of freedom to ensure deformation occurs only within the actual shear connector link that spans the 60 mm (2.4 in.) distance between the two rigid arms (Fig. 7). The shear connector link was assigned stiffness in the U2 direction, representing the shear stiffness $K_{c,i}$ of the connection system (details of this stiffness are provided later).

Similar to the rigid foam (insulation) link, the shear connector link was also fixed vertically (direction U1). The other four degrees of freedom for this link (U3, R1, R2, and R3) had zero assigned stiffness. Loads were applied to the upper wythe element on either side of the midspan, creating a constant moment zone of 550 mm (22 in.), identical to that of the experimental procedure. The total slip from the structural analysis model was determined using the horizontal translation of the end nodes of the rigid link elements modeling the insulation-concrete interface. The total slip is the slip of node 1 coupled with the projected slip of node 2 at the level of node 1 or vice versa. To model a theoretically fully noncomposite panel, the U2 stiffness of the shear connector link is set to zero. A fully composite panel is modeled as a single wythe beam element with rotational one-joint links for the semi-rigid supports (Fig. 7) without shear connectors or rigid foam (insulation) link elements.

Moment-curvature responses

Using the wythe dimensions, reinforcement details, and material properties described earlier, the moment-curvature responses of facade and structural wythes were established using a sectional analysis computer program. For a given curvature, a secant is drawn from zero to the corresponding moment on the moment-curvature plot (**Fig. 8**). The slope of the secant is the stiffness EI_i of the wythe for that particular curvature. Assuming an arbitrary modulus of elasticity E_i and a square cross section, the dimensions of the idealized wythe can be determined using the moment of inertia I_i and entered into the structural analysis model for the cord members.

Shear connection model

The stiffness of the specified shear connector system was determined using the experimental data from push-through tests on identical connector layouts.[9] **Figure 9** shows a schematic of the push-through specimen. The load-slip relationship is equivalent to that of a linear spring system with a linear stiffness $K_{c,i}$ (Fig. 9). The linear spring

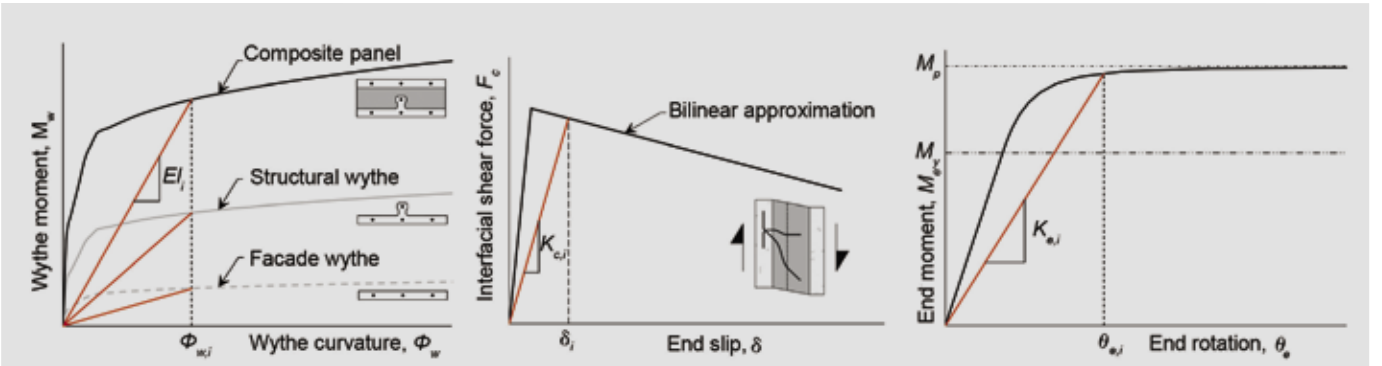

Figure 8. Critical element properties and stiffness determination. Note: EI_i = stiffness at load stage i; $K_{c,i}$ = linear stiffness of shear connection system at load stage i; $K_{e,i}$ = rotational end stiffness at load stage i; M_p = internal plastic moment of angle; M_y = internal yield moment of angle; δ_i = relative slip between wythes at load stage i; $\theta_{e,i}$ = end rotation at load stage i; $\phi_{w,i}$ = midspan wythe curvature at load stage i.

in actuality is a shear spring, as the top wythe translates longitudinally relative to the bottom wythe (Fig. 9). For a given slip between wythes δ_i, the linear stiffness $K_{c,i}$ is the slope of a secant drawn from zero to the corresponding interfacial shear force $F_{c,i}$ (Fig. 8). A simplified bilinear curve was fit to the experimental load-slip data (Fig. 9).

Moment-rotation models

Unique moment-rotation relationships for the bolted angle connections have been developed for both the pressure and suction loading configurations. The analysis of the pressure configuration (**Fig. 10**) assumes an L-shaped cantilever mechanism for the angle with the fixed end located at the centerline of the bolt in the vertical leg (Fig. 10). The reaction force from panel self-weight and applied loading is approximated as a distributed load across the horizontal angle leg. Figure 10 shows the development of the rotation geometry and resulting total rotation of connection system in pressure configuration θ_c. The individual rotations are determined by integrating the curvature distribution on each leg, which is inferred using the moment distribution and inherent moment-curvature relationship for the angle cross section (Fig. 10). The resulting moment-rotation relationship closely follows that of the moment-curvature plot, with the curve ultimately leveling off at the plastic moment M_p asymptote (Fig. 8). For a given end rotation $\theta_{e,i}$, the rotational end stiffness $K_{e,i}$ is the slope of a secant drawn from zero to the corresponding end moment $M_{e,i}$.

The analysis of the suction configuration also assumes a cantilever mechanism for the angle with the fixed end located at the centerline of the bolt in the vertical leg (**Fig. 11**). However, the resulting rotation of the system occurs about a pivot point at the interface of the grout and the lower corner of the thickened panel header (Fig. 11). The rotation of the panel is triggered by the horizontal force F_a, which causes free-end deflection of the vertical cantilever leg. Because the height of the header is constant, the total rotation of the system in suction configuration θ_d is a function of the free-end angle deflection Δ_a and height of the header in the structural wythe h (Fig. 11). Similar to the pressure moment-rotation model, the deflection of the cantilever free end is determined by double integrating the curvature distribution (Fig. 11). A moment-rotation curve is then produced.

Procedure of analysis

To obtain the load deflection, load-end slip, and load-end rotation responses of partially composite sandwich wall

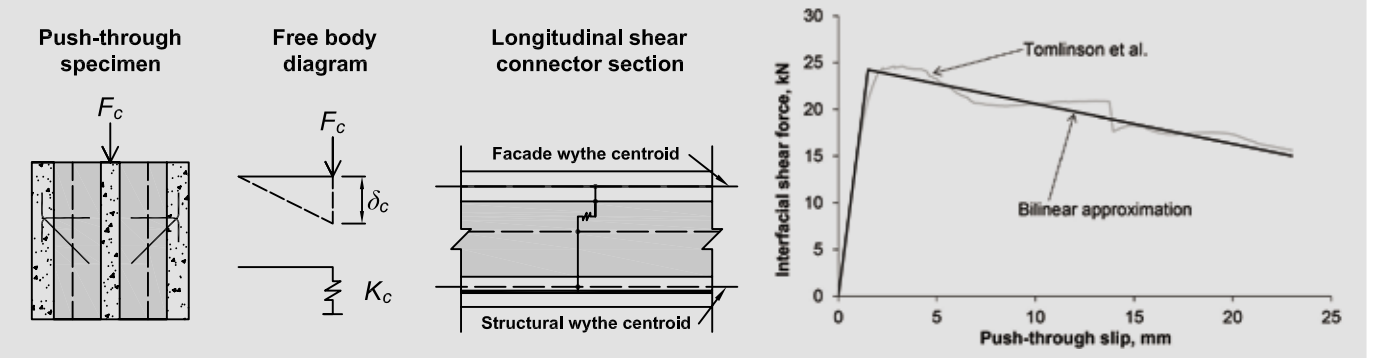

Figure 9. Shear connector stiffness model development. Note: F_c = interfacial shear force; K_c = linear stiffness of shear connection system; δ_c = relative slip between wythes in push-through tests. 1 mm = 0.0394 in.; 1 kN = 0.225 kip.

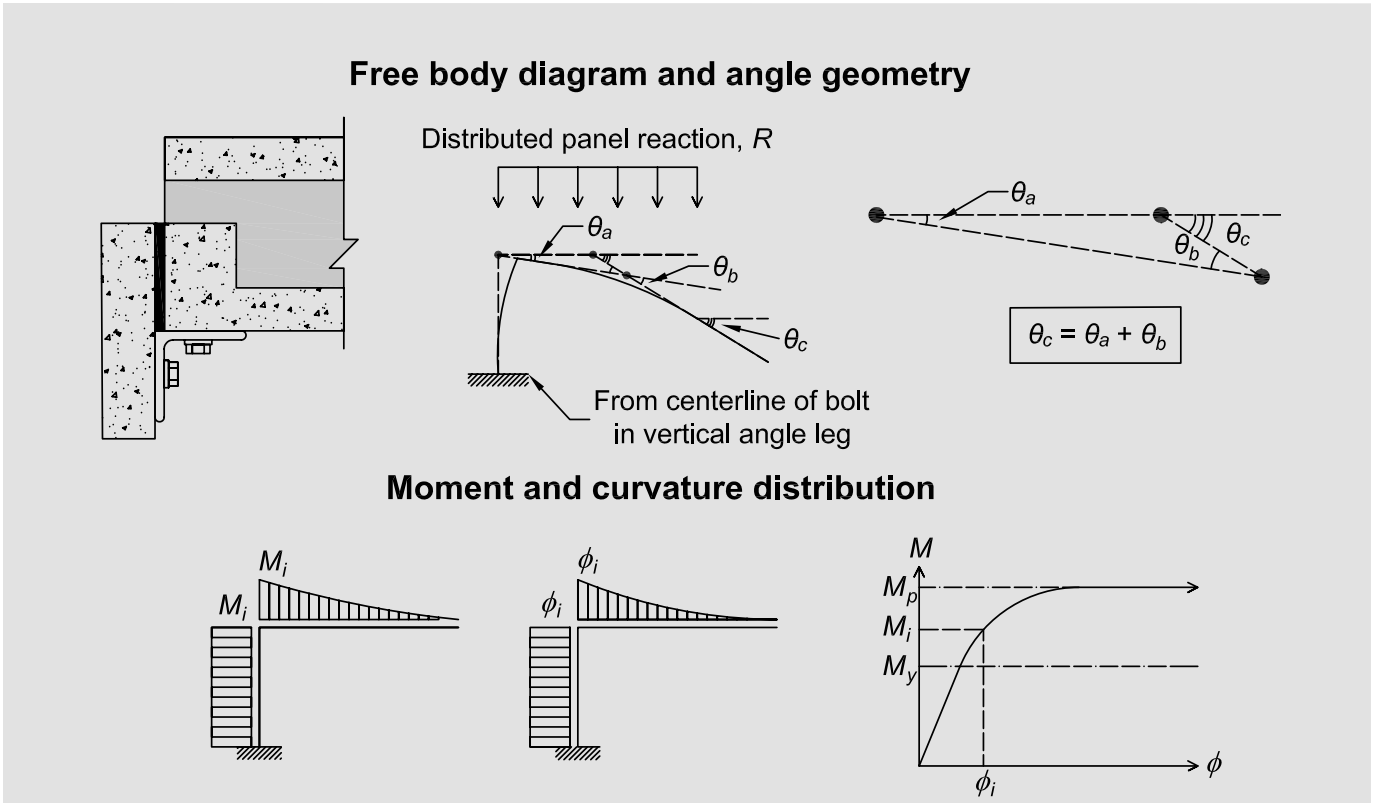

Figure 10. Moment-rotation model development for bolted angle connection in pressure configuration. Note: M = moment; M_i = moment at load stage i; M_p = internal plastic moment of angle; M_y = internal yield moment of angle; θ_a = rotation of vertical leg of angle in pressure configuration; θ_b = rotation of horizontal leg of angle in pressure configuration; θ_c = total rotation of connection system in pressure configuration; ϕ = wythe curvature; ϕ_i = wythe curvature at load stage i.

panels, the procedure can be summarized in the following steps:

1. Specify the desired wythe dimensions, reinforcement details, and material properties in the sectional analysis computer program to obtain the moment-curvature response for each individual wythe.

2. For a given applied load, assume a value for midspan deflection Δ.

3. Using the estimated midspan deflection Δ, calculate a corresponding wythe midspan curvature $\phi_{w,i}$ using Eq. (1),[18] where end curvatures are assumed to be negligible compared with the midspan and ℓ is the span length:

$$\Delta = \frac{\ell^2}{96}\left(10\phi_{w,i}\right) \quad (1)$$

4. From the moment-curvature responses for the structural and facade wythes, determine the moment resistance of wythe $M_{w,i}$ and stiffness (slope) EI_i for each wythe corresponding to the wythe midspan curvature $\phi_{w,i}$ (Fig. 8). It is assumed that both wythes always have the same curvature.

5. Assuming an arbitrary modulus of elasticity E_i, back calculate the dimensions of each equivalent square wythe using the moment of inertia I_i, to be entered in the structural analysis software model in step 10.

6. Assume values for relative slip between wythes δ_i at the locations of inner and outer shear connectors.

7. From the shear connector load-slip plot, determine the linear stiffness of the shear connection system (slope) $K_{c,i}$ for each connector corresponding to the estimated slip values δ_i (Fig. 9), to be entered in the structural analysis model in step 10.

8. If the panel has semi-rigid supports, assume a value for end rotation at the supports $\theta_{e,i}$.

9. From the support moment-rotation plot, determine the rotational end stiffness (slope) $K_{e,i}$ corresponding to the estimated support rotation $\theta_{e,i}$, to be entered in the structural analysis model in step 10. If the support is hinged rather than semirigid, the stiffness is zero.

10. Input the wythe dimensions (equivalent square), inner- and outer-connector stiffness, and support stiffness

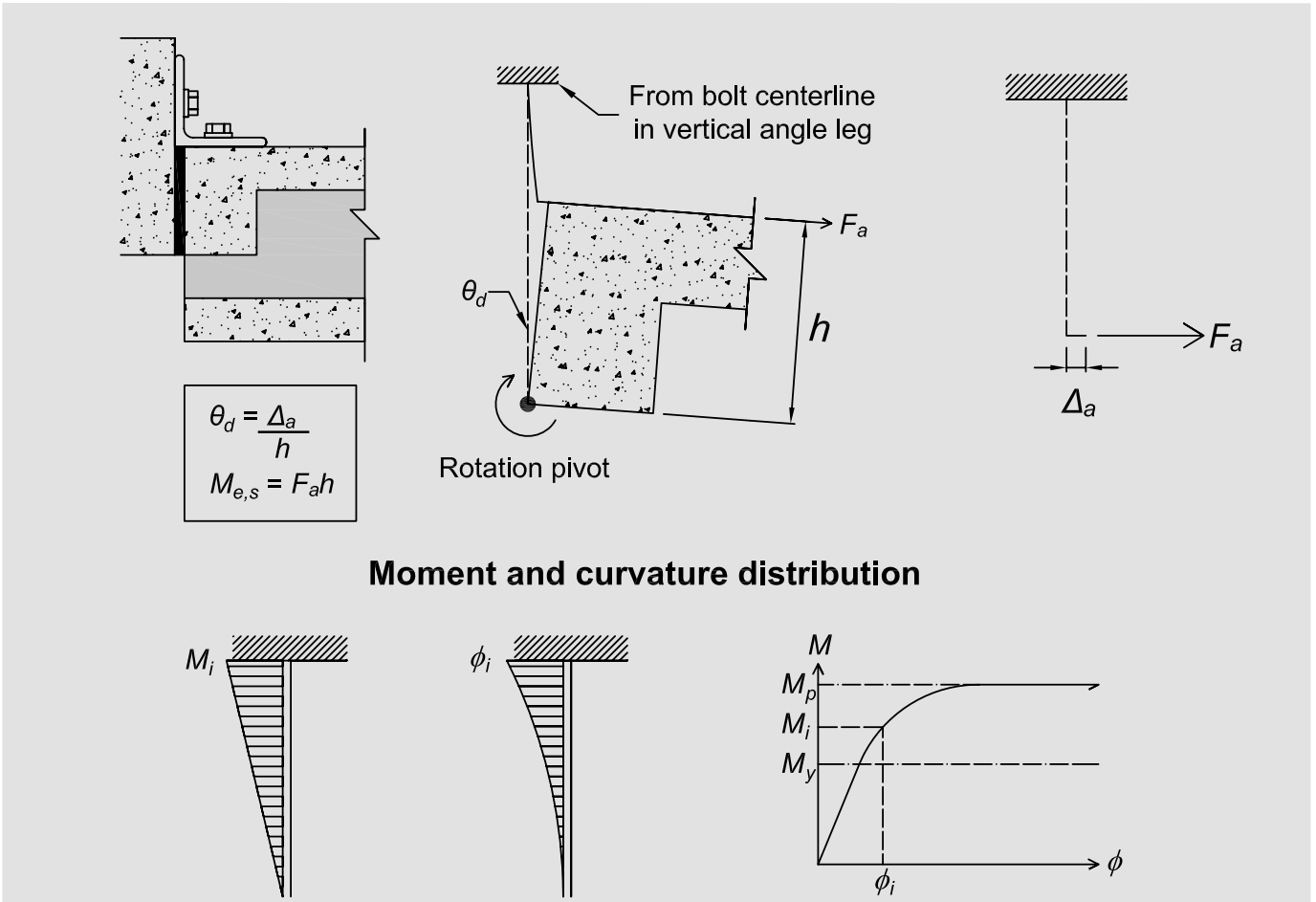

Figure 11. Moment-rotation model development for bolted angle connection in suction configuration. Note: F_a = applied force at free end of vertical leg of angle in suction configuration; h = height of header in structural wythe; M = moment; $M_{e,s}$ = end moment in suction configuration; M_i = moment at load stage i; M_p = internal plastic moment of angle; M_y = internal yield moment of angle; Δ_a = free-end deflection of vertical leg of angle in suction configuration; θ_d = total rotation of connection system in suction configuration; ϕ = wythe curvature; ϕ_i = wythe curvature at load stage i.

into the structural analysis software model, and run the analysis under the applied load assumed in step 2.

11. Record the resulting midspan deflection, support rotation, and relative slip between wythes at the location of the outer and inner shear connectors.

12. Calculate a new curvature using the resulting midspan deflection as well as the corresponding moments, stiffness, and wythe dimensions for each wythe using steps 3 to 5.

13. Calculate a new stiffness value for the inner and outer shear connectors corresponding to the structural analysis software slip outputs as outlined in step 7.

14. Calculate a new stiffness value for the supports corresponding to the structural analysis software rotation output as outlined in step 9.

15. Input the new wythe dimensions, outer- and inner-connector stiffness, and support stiffness into structural analysis software and rerun the analysis under the same load assumed in step 2.

16. Repeat steps 12 to 15 until the deflection, inner- and outer-connector slip, and support rotation output and input values converge completely.

17. In addition to the final output values, record the internal moment at the location of the support.

18. Proceed to the next loading level in step 2 and repeat this process until one of the wythes has reached its ultimate moment resistance and corresponding curvature or until the shear connection system fails.

The structural analysis model can also produce the upper and lower bounds of composite and noncomposite panels. To obtain the fully noncomposite responses, the same procedure is used but a zero stiffness value is assigned for the shear connection. Complete the remainder

of the procedure until the convergence of the midspan deflection and support rotation. Upon completion, record the resulting inner- and outer-connector slip in addition to the support moment. For a fully composite panel, rather than modeling two wythe elements, a single beam element is used to model the fully composite nature of the section. Under this configuration there are no shear connector link elements. Complete the procedure until the convergence of midspan deflection and support rotation.

Verification of model

The model has been used to predict the flexural behavior of specimens W1 to W3 and L1 to L3 in terms of load deflection, load-end slip, and load-end rotation. Figures 1 and 2 show the layout and cross-sectional details of the specimens. For specimens W3 and L3, cast horizontally and with BFRP reinforcement, an additional prediction was developed to model the absence of insulation-concrete bond adhesion. This was accounted for in the load-slip model by fitting data from push-through tests (Fig. 9) with bond breaker.[9] **Figure 12** shows the predicted responses of all panels. The predicted fully composite and noncomposite responses are also depicted. In general, the model predicts the partially composite stiffness reasonably well but tends to underestimate the ultimate strength of steel-reinforced panels (that is, it is on the conservative side) and overestimate end slip. For BFRP-reinforced panels, the prediction ignoring insulation-concrete bond shows better agreement with test results.

There are two potential explanations for the conservative nature of the model. First, the shear connector model developed from the push-through tests does not include the effect of the panel curvature in flexure. (That is, the applied push-through load acted parallel to the wythes, whereas the applied load in the full-scale flexural tests acted perpendicular to the panel.) Second, the applied loads and reactions on the full-scale panels compressed the panel cross section transversely, thereby increasing the magnitude of friction at the insulation-concrete interface and resulting in higher shear transfer. These two notions may explain the discrepancy in peak load and end slip between the predicted and the experimental responses.

Amount of composite action

Table 2 quantifies the amount of composite action of test panels (as a percentage) according to the relationship given in Eq. (2), defined by Tomlinson et al.[19]

$$\kappa = \frac{P_{u,exp} - P_{u,nc}}{P_{u,c} - P_{u,nc}} \times 100\% \qquad (2)$$

where

κ = percentage of composite action

$P_{u,exp}$ = peak experimental load

$P_{u,nc}$ = peak noncomposite load predicted by the model

$P_{u,c}$ = peak fully composite load predicted by the model

Steel-reinforced, pressure-loaded specimens W1 and L1 achieved 81% to 88% composite action, while BFRP-reinforced, pressure-loaded specimens W3 and L3 reached only 21% to 29% composite action at peak loading. Suction-loaded, steel-reinforced specimens W2 and L2 achieved 57% to 66% composite action, about 20% less than their respective counterparts tested in pressure. The effect of support condition on degree of composite action is insignificant compared with loading direction and reinforcement type.

Conclusion

The following conclusions may be drawn from the experimental and analytical studies on concrete sandwich wall panels and the effects of support condition, loading direction, and reinforcement material:

- The bolted angle connections did not fail and succeeded in developing the full strength of the sandwich wall panels. Steel-reinforced panels failed by fracture of the flexure steel reinforcement, whether loaded in pressure or suction. The bolted angle connection was generally intact, except for some yielding in the angle. BFRP-reinforced panels failed by fracture of the BFRP shear connectors followed by crushing of the concrete web of the structural wythe.

- Bolted angle connections contribute stiffness to the sandwich wall panel system and increase the overall structural capacity regardless of loading direction and reinforcement type by 15% to 33% compared with roller supports. The introduction of partial fixity and some negative moments at the ends reduces the structural demand at midspan, allowing the panel to resist higher loads. The added stiffness allows the panel to reach its peak load at a lower deflection and end rotation than its simply supported counterpart.

- The bolted angle panels loaded in a configuration that simulates external wind pressure achieved 25% higher peak loads than when loaded from the opposite direction simulating suction. When both configurations were supported by rollers, this increase was 40%.

- The bolted angle panel reinforced with BFRP flexural reinforcement and connectors with a reinforcement

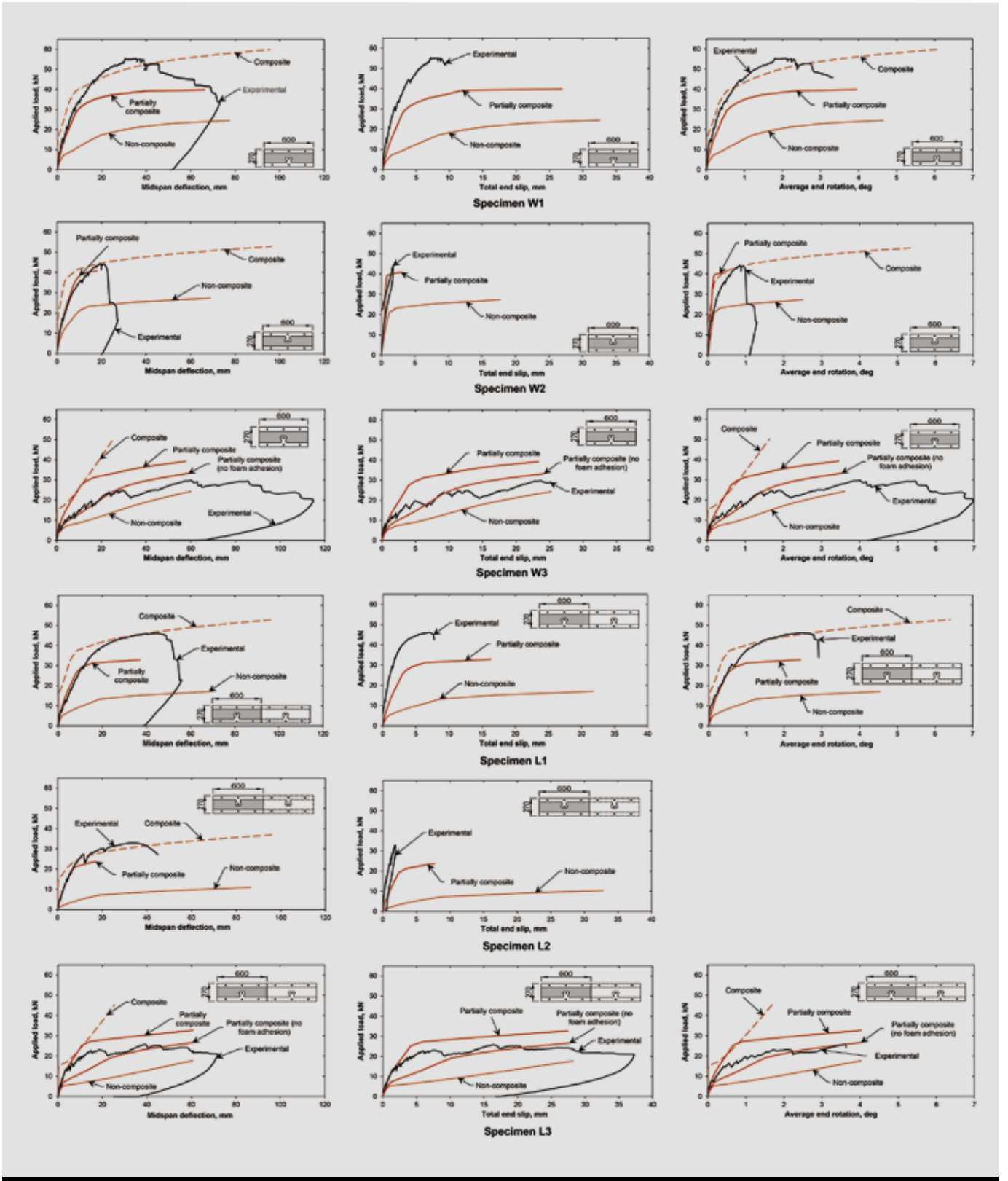

Figure 12. Predicted versus experimental responses of partially composite concrete sandwich wall panels. Note: 1 mm = 0.0394 in.; 1 kN = 0.225 kip.

ratio similar to its steel-reinforced counterpart showed 33% lower capacity. Insulation-concrete bond in the BFRP panel, however, was lower due to horizontal, rather than vertical, casting.

- Steel-reinforced, pressure-loaded specimens achieved 81% to 88% composite action, while BFRP-reinforced, pressure-loaded specimens reached only 21% to 29% composite action at peak loading. Suction-

loaded, steel-reinforced specimens achieved 57% to 66% composite action, about 20% less than their respective counterparts tested in pressure. The effect of support condition on degree of composite action was insignificant compared with loading direction and reinforcement type.

- An analytical approach for predicting the partial composite response of sandwich wall panels was developed and validated with experimental results. The model accounts for concrete and steel nonlinearity, cracking, a bond-slip model for shear connection, and a moment-rotation model for partial end fixity. The model predicts flexural stiffness well but tends to underestimate ultimate loads (that is, it is generally on the conservative side).

References

1. PCI Committee on Precast Sandwich Wall Panels. 1997. "State-of-the-Art of Precast/ Prestressed Sandwich Wall Panels." *PCI Journal* 42 (2): 92–134.

2. CPCI (Canadian Precast/Prestressed Concrete Institute). 2012. *Insulated Wall Precast Concrete*. Technical brochure. Ottawa, ON, Canada: CPCI.

3. PCI Committee on Precast Sandwich Wall Panels. 2011. "State of the Art of Precast/Prestressed Concrete Sandwich Wall Panels." *PCI Journal* 56 (2): 131–176.

4. Frankl, B., G. Lucier, T. Hassan, and S. H. Rizkalla. 2011. "Behavior of Precast, Prestressed Concrete Sandwich Wall Panels Reinforced with CFRP Grid." *PCI Journal* 56 (2): 42–54.

5. McCall, W. C. 1985. "Thermal Properties of Sandwich Panels." *Concrete International* 7 (1): 35–41.

6. Soriano, J., and S. H. Rizkalla. 2013. "Use of FRP Grid for the Composite Action of Concrete Sandwich Panels." In *11th International Symposium on Fiber Reinforced Polymer for Reinforced Concrete Structures: Proceedings, June 26–28, 2013, Guimarães, Portugal*. Guimarães, Portugal: University of Minho.

7. Frankl, B. 2008. "Structural Behavior of Insulated Precast Prestressed Concrete Sandwich Panels Reinforced with CFRP Grid." MSc thesis, Department of Civil, Construction and Environmental Engineering, North Carolina State University, Raleigh, NC.

8. Naito, C. J., M. Beacraft, J. M. Hoemann, and B. T. Bewick. 2012. "Performance and Characterization of Shear Ties for Use in Insulated Precast Concrete Sandwich Wall Panels." *Journal of Structural Engineering* 138 (1): 52–61.

9. Tomlinson, D. G., N. Teixeira, and A. Fam. 2016. "New Shear Connector Design for Insulated Concrete Sandwich Panels using Basalt Fiber Reinforced Polymer Bars." *Journal of Composites for Construction*. doi: 10.1061/(ASCE)CC.1943-5614.0000662.

10. Pang, S. C. 2002. "A Study of In-Situ L-Connections for Precast Concrete Sandwich Panels." MSc thesis, University Putra Malaysia, Seri Kembangan, Malaysia.

11. Benayoune, A., A. A. A. Samad, D. N. Trikha, A. A. A. Ali, and A. M. Akhand. 2004. "Precast Reinforced Concrete Sandwich Panel as an Industrialised Building System." In *8th International Conference on Concrete Engineering and Technology (CONCET 2004): Proceedings, April 19–21, 2004, Langkawi Island, Malaysia*. Kuala Lumpur: University of Malaya.

12. Carbonari, G., S. H. P. Cavalaro, M. Cansario, and A. Aguado. 2012. "Flexural Behaviour of Light-Weight Sandwich Panels Composed by Concrete and EPS." *Construction and Building Materials* no. 35: 792–799.

13. Metelli, G., and P. Riva. 2007. "Behaviour of a Support System for Pre-cast Concrete Panels." In *Fracture Mechanics of Concrete and Concrete Structures: Proceedings of the 6th International Conference on Fracture Mechanics of Concrete and Concrete Structures, Catania, Italy, 17–22 July 2007*. Boca Raton, FL: CRC Press.

14. Holmes, W. W., D. Kusolthamarat, and M. K. Tadros. 2005. "NU Precast Concrete House Provides Spacious and Energy Efficient Solution for Residential Construction." *PCI Journal* 50 (3): 16–25.

15. Tomlinson, D. G., and A. Fam. 2015. "Flexural Behavior of Precast Concrete Sandwich Panels with Basalt-FRP and Steel Reinforcement." *PCI Journal* 60 (6): 51–71.

16. ACI (American Concrete Institute) Committee 318. 2014. *Building Code Requirements for Structural Concrete (ACI 318-14) and Commentary (ACI 318R-14)*. Farmington Hills, MI: ACI.

17. ASTM International. *Standard Specification for Structural Bolts, Steel, Heat Treated, 120/105 ksi, Minimum Tensile Strength*. ASTM A325-14. West Conshohocken, PA: ASTM.

18. Ghali, A., R. Favre, and M. Elbadry. 2006. *Concrete Structures: Stresses and Deformations: Analysis and Design for Serviceability*. Boca Raton, FL: CRC Press.

19. Tomlinson, D. G., N. Teixeira, and A. Fam. 2014. "Comparison of Steel and BFRP Shear Connectors in Insulated Precast Concrete Wall Panels." In *The 60th Anniversary PCI Convention and National Bridge Conference: Proceedings, September 6–9, 2014, Washington, D.C.* Chicago, IL: PCI. CD-ROM.

Notation

E_i = elastic modulus at load stage i

EI_i = stiffness at load stage i

f_c' = specified compressive strength of concrete

f_y = yield strength

F_a = applied horizontal force at free end of vertical leg of angle in suction configuration

F_c = interfacial shear force

$F_{c,i}$ = interfacial shear force at load stage i

h = height of header in structural wythe

I_i = moment of inertia at load stage i

K_c = linear stiffness of shear connection system

$K_{c,i}$ = linear stiffness of shear connection system at load stage i

$K_{e,i}$ = rotational end stiffness at load stage i

ℓ = span length

M = moment

M_e = end moment

$M_{e,i}$ = end moment at load stage i

$M_{e,s}$ = end moment in suction configuration

M_i = moment at load stage i

M_p = internal plastic moment of angle

M_w = moment resistance of wythe

$M_{w,i}$ = moment resistance of wythe at load stage i

M_y = internal yield moment of angle

$P_{u,c}$ = peak fully composite load predicted by the model

$P_{u,exp}$ = peak experimental load

$P_{u,nc}$ = peak noncomposite load predicted by the model

δ = relative slip between wythes

δ_c = relative slip between wythes in push-through test

δ_i = relative slip between wythes at load stage i

Δ = midspan deflection

Δ_a = free-end deflection of vertical leg of angle in suction configuration

θ_a = rotation of vertical leg of angle in pressure configuration

θ_b = rotation of horizontal leg of angle in pressure configuration

θ_c = total rotation of connection system in pressure configuration

θ_d = total rotation of connection system in suction configuration

θ_e = end rotation

$\theta_{e,i}$ = end rotation at load stage i

κ = percentage of composite action

ϕ = wythe curvature

ϕ_i = wythe curvature at load stage i

ϕ_w = midspan wythe curvature

$\phi_{w,i}$ = midspan wythe curvature at load stage i

About the authors

Nathan Teixeira, MS, earned his master's degree in civil engineering in November 2015 from Queen's University in Kingston, ON, Canada. He is currently working for Stantec in the greater Toronto area.

Douglas G. Tomlinson, PhD, is a postdoctoral fellow in the Department of Civil Engineering at Queen's University. He earned his PhD in November 2015.

Amir Z. Fam, PhD, PEng, is a professor and the Donald and Sarah Munro Chair in Engineering and Applied Science in the Department of Civil Engineering at Queen's University.

Abstract

In this study, flexural tests were performed on precast concrete sandwich wall panels with various end support conditions, loading orientations, and reinforcement and shear connector materials. Bolted angle connections were used to simulate practical support conditions while loads were applied in a manner to simulate windward pressure as well as suction. Panels with steel and basalt-fiber-reinforced polymer (BFRP) longitudinal reinforcement were tested and compared. Discrete steel and BFRP shear connectors were also used and evaluated. The bolted angle connections provided partial end fixity, thereby increasing the overall strength and stiffness relative to identical panels simply supported by rollers during testing. In all cases the bolted connections succeeded in developing the full strength of the sandwich wall panels. Panels with steel reinforcement failed due to rupturing of flexural reinforcement, while a panel with BFRP reinforcement failed due to rupturing of shear connectors and crushing of concrete in one wythe. Panels loaded in the direction of wind pressure achieved higher peak loads than identical panels loaded to simulate suction. An independent analytical model accounting for material nonlinearity, end support conditions, and partial composite action from the shear transfer system was developed. The model accurately predicted flexural stiffness, while the peak load was underestimated in most cases.

Keywords

Analytical model, basalt-fiber-reinforced polymer, BFRP, composite action, connection, flexural test, panel, sandwich wall, shear connector.

Review policy

This paper was reviewed in accordance with the Precast/Prestressed Concrete Institute's peer-review process.

Reader comments

Please address reader comments to journal@pci.org or Precast/Prestressed Concrete Institute, c/o *PCI Journal*, 200 W. Adams St., Suite 2100, Chicago, IL 60606.